Inorg. Chem. **2007**, *46*, 9337−9350

Charge Separation in a Ruthenium-Quencher Conjugate Bound to DNA

Katherine E. Augustyn, E. D. A. Stemp,† and Jacqueline K. Barton*

Division of Chemistry and Chemical Engineering, California Institute of Technology, Pasadena, California 91125

Received June 28, 2007

A novel tris heteroleptic dipyridophenazine complex of ruthenium(II), [{Ru(phen)(dppz)(bpy′-his)}{Ru(NH_3)$_5$}]$^{5+}$, containing a covalently tethered ruthenium pentammine quencher coordinated through a bridging histidine has been synthesized and characterized spectroscopically and biochemically in a DNA environment and in organic solvent. Steady-state and time-resolved luminescence measurements indicate that the tethered Ru complex is quenched relative to the parent complexes [Ru(phen)(dppz)(bpy′)]$^{2+}$ and [Ru(phen)(dppz)(bpy′-his)]$^{2+}$ in DNA and acetonitrile, consistent with intramolecular photoinduced electron transfer. Intercalated into guanine-containing DNA, [{Ru(phen)(dppz)(bpy′-his)}{Ru(NH_3)$_5$}]$^{5+}$, upon excitation and intramolecular quenching, is capable of injecting charge into the duplex based upon the EPR detection of guanine radicals. DNA-mediated charge transport is also indicated using a kinetically fast cyclopropylamine-substituted base as an electron hole trap. Guanine damage is not observed, however, in measurements using the guanine radical as the kinetically slower hole trap, indicating that back electron-transfer reactions are competitive with guanine oxidation. Moreover, transient absorption measurements reveal a novel photophysical reaction pathway for [{Ru(phen)(dppz)(bpy′-his)}{Ru(NH_3)$_5$}]$^{5+}$ in the presence of DNA that is competitive with the intramolecular flash-quench process. These results illustrate the remarkably rich redox chemistry that can occur within a bimolecular ruthenium complex intercalated in duplex DNA.

Introduction

It is well established that the π-stack of the DNA double helix can serve as an efficient medium for charge transport.[1−5] With reactions spanning distances over 200 Å, this process is acutely sensitive to the intervening bridging bases.[6,7] A well-coupled π-stack facilitates efficient charge transport reactions with a shallow distance dependence and can result in permanent oxidative DNA base damage. Oxidative base lesions resulting from DNA-mediated charge transport reactions are particularly relevant in the field of aging and in many diseases, including cancer and neurodegenerative disorders.[8−10] Guanine, with the lowest oxidation potential of the naturally occurring bases, can effectively serve as a hole trap.[11] Upon oxidation, the guanine cation radical can react with water to form the permanent damage product 8-oxo-7,8-dihydro-2′-deoxyguanosine (8-oxo-dG) or rapidly deprotonate to form the neutral radical, which reacts irreversibly on a longer time scale (>ms) with oxygen to form permanent damage products such as oxazolone and imidazolone.[12] While biochemical techniques to probe guanine damage yields at long range have been auspicious in underscoring the exquisite sensitivity of charge transport to base stacking and sequence, because of the slow trapping rate of the guanine radical, these studies are inevitably

* To whom correspondence should be addressed. E-mail: jkbarton@caltech.edu.

† Current address: Department of Physical Sciences, Mt. Saint Mary's College, Los Angeles, CA 90049.

(1) Delaney, S.; Barton, J. K. *J. Org. Chem.* **2003**, *68*, 6475−6483.
(2) Schuster, G. B. *Acc. Chem. Res.* **2000**, *33*, 253−260.
(3) Giese, B. *Annu. Rev. Biochem.* **2002**, *71*, 51−70.
(4) Lewis, F. D.; Letsinger, R. L.; Wasielewski, M. R. *Acc. Chem. Res.* **2001**, *34*, 159−170.
(5) Kawai, K.; Takada, T.; Tojo, S.; Ichinose, N.; Majima, T. *J. Am. Chem. Soc.* **2001**, *123*, 12688−12689.
(6) Nuñez, M. E.; Hall, D. B.; Barton, J. K. *Chem. Biol.* **1999**, *6*, 85−97.
(7) Ly, D.; Sanii, L.; Schuster, G. B. *J. Am. Chem. Soc.* **1999**, *121*, 9400−9410.
(8) Kelley, S. O.; Barton, J. K. Radical *Metal Ions Biol.* **1999**, *35*, 211−249.
(9) Wiseman, H.; Halliwell, B. *Biochem. J.* **1996**, *313*, 17−29.
(10) Ames, B. N.; Shigenaga, M. K.; Hagen, T. M. *Proc. Natl. Acad. Sci. U.S.A.* **1993**, *90*, 7915−7922.
(11) Steenken, S.; Jovanovic, S. V. *J. Am. Chem. Soc.* **1997**, *119*, 617−618.
(12) (a) Candeias, L.; Steenken, S. *Chem.—Eur. J.* **2000**, *6*, 475−484. (b) Steenken, S. *Free Radical Res. Commun.* **1992**, *16*, 349. (c) Shafiovich, V.; Cadet, J.; Gasparutto, D.; Dourandin, A.; Huang, W.; Geacintov, N. E. *J. Phys. Chem. B* **2001**, *105*, 586.

10.1021/ic701276t CCC: $37.00
Published on Web 10/02/2007

convoluted by processes such as back electron transfer and hence provide information several steps removed from the initial transport event.[13]

Elucidation of the kinetics of charge transport through DNA is fundamental to characterization of this process. Previous studies have measured the charge transport rates through relatively short DNA assemblies using techniques such as pulse radiolysis[14] and transient absorption spectroscopy.[15,16] However, these studies probe transport using external reporters and do not directly detect base radicals. Although guanine oxidation can be detected spectroscopically because of the characteristic absorption of its radical centered at 390 nm, the small extinction coefficient of the guanine radical can pose a significant challenge in delineating the charge transport rates, particularly, if the absorption overlaps with that of the photooxidant.[17]

Our laboratory has extensively studied DNA charge transport reactions using rhodium and ruthenium intercalators as photooxidants.[18] These complexes are ideal probes for charge transport reactions because of the strong electronic coupling between the intercalating ligand and the DNA π-stack. Both the phenanthrenequinone diimine (phi) complexes of rhodium(III) and the dipyridophenazine (dppz) complexes of ruthenium(II) bind avidly to DNA and can be used to probe charge transport through DNA.[19] Irradiation of the DNA-bound metal complex generates a potent photooxidant capable of injecting charge into the base stack and the resulting oxidation reaction can be revealed using biochemical techniques. More recently these complexes have served as potent photooxidants in charge-transport studies using cyclopropylamine-substituted bases as hole traps.[20] With irreversible oxidative ring opening occurring on the picosecond time scale, cyclopropylamine-subsituted nucleosides provide a means to delineate hole transport on time scales competitive with back electron transfer.[13,20−23] The dppz complexes of ruthenium(II) have an added advantage in that they can be used to probe spectroscopically charge transport kinetics using a modified flash-quench technique providing a comparison to biochemical techniques.[24]

First developed to study high driving force reactions in cytochrome c,[25] flash-quench methodologies have been modified to monitor rates of guanine radical formation in DNA.[19,24,26] Here, the Ru(II) excited state is localized on the intercalated dppz ligand, and upon oxidation with an externally bound quencher such as $[Ru(NH_3)_6]^{3+}$, methyl viologen, or $[Co(NH_3)_5Cl]^{2+}$, a powerful Ru(III) ground-state oxidant capable of oxidizing guanine is generated *in situ*. Limits on the rates of hole injection into the duplex and rates of transport between Ru(III) and guanine can thus be determined by monitoring the transiently generated guanine radical.

Previously our laboratory used this flash-quench technique to measure rates of DNA-mediated charge transport between the artificial base 4-methylindole and the tris heteroleptic ruthenium complex, $[Ru(phen)(dppz)(bpy')]^{2+}$.[27,28] The artificial base was used in place of a selected guanine residue in this study because of the favorable spectroscopic properties of its radical, the low oxidation potential of methylindole ($\sim$1.0 V vs NHE), and the ability to fix effectively the distance between the donor and acceptor without interference from additional guanines. Interestingly, regardless of the sequence or the distance between the donor and acceptor, all rates of methylindole radical formation were found to be on the order of 10^7 s^{-1}, coincident with the rate of Ru(III) generation. Essentially, as soon as the Ru(III) oxidant is generated, the hole is transported down the DNA stack to form the methylindole radical cation. Importantly, in this flash-quench reaction, the rate of Ru(III) formation depends upon diffusion of the quencher. Thus, in this system, diffusional quenching is rate limiting.

To measure rates occurring on a faster time scale than that of diffusional quenching, we have developed a system in which the quencher is covalently tethered to the ruthenium complex, effectively eliminating the rate-limiting quenching step. Several groups have covalently tethered quencher moieties to ruthenium complexes. One study showed that a viologen-tethered ruthenium complex exhibits a long-lived charge separated state and is able to photocleave DNA under inert atmosphere.[29] In another study, intramolecular electron transfer was observed between ruthenium complexes covalently tethered to quenchers through Schiff base bridges.[30] Intermolecular quenching has also been observed in ruthe-

(13) Williams, T. T.; Dohno, C.; Stemp, E. D. A.; Barton, J. K. *J. Am. Chem. Soc.* **2004**, *126*, 8148−8158.
(14) Kawai, K.; Kimura, T.; Kawabata, K.; Tojo, S.; Majima, T. *J. Phys. Chem. B* **2003**, *107*, 12838−12841.
(15) Takada, T.; Kawai, K.; Tojo, S.; Majima, T. *J. Phys. Chem. B* **2003**, *107*, 4052−12057.
(16) Lewis, F. D.; Liu, X.; Liu, J.; Miller, S. E.; Hayes, T. R.; Wasielewski, M. R. *Nature* **2000**, *406*, 51−53.
(17) Nguyen, K. L.; Steryo, M.; Kurbanyan, K.; Nowitzki, K. M.; Butterfield, S. M.; Ward, S. R.; Stemp, E. D. A. *J. Am. Chem. Soc.* **2000**, *122*, 3585−3594.
(18) Augustyn, K. E.; Pierre, V. C.; Barton, J. K. *Wiley Encylopedia Chem. Biol.* **2007**, in press.
(19) (a) Erkkila, K. E.; Odom, D. T.; Barton, J. K. *Chem. Rev.* **1999**, *99*, 2777−2795. (b) Arkin, M. R.; Stemp, E. D. A.; Pulver, S. C.; Barton, J. K. *Chem. Biol.* **1997**, *4*, 389−400. (c) Hall, D. B.; Holmlin, R. E.; Barton, J. K. *Nature* **1996**, *382*, 731−735.
(20) Shao, F.; Augustyn, K. E.; Barton, J. K. *J. Am. Chem. Soc.* **2005**, *127*, 17445−17452.
(21) (a) Nakatani, K.; Dohno, C.; Saito, I. *J. Am. Chem. Soc.* **2001**, *123*, 9681−9682. (b) O'Neill, M. A.; Dohno, C.; Barton, J. K. *J. Am. Chem. Soc.* **2004**, *126*, 1316−1317.
(22) Shao, F.; O. Neill, M. A.; Barton, J. K. *Proc. Natl. Acad. Sci. U.S.A.* **2004**, *101*, 17914−17919.
(23) Musa, O. M.; Horner, J. H.; Shahin, H.; Newcomb, M. *J. Am. Chem. Soc.* **1996**, *118*, 3862−3868.
(24) Stemp, E. D. A.; Arkin, M. R.; Barton, J. K. *J. Am. Chem. Soc.* **1997**, *119*, 2921−2925.
(25) Chang, J. I.; Gray, B. H.; Winkler, J. R. *J. Am. Chem. Soc.* **1991**, *113*, 7056−7057.
(26) Dunn, D. A.; Lin, V. H.; Kochevar, I. E. *Biochemistry* **1992**, *31*, 11620−11625.
(27) Pascaly, M.; Yoo, J.; Barton, J. K. *J. Am. Chem. Soc.* **2002**, *124*, 9083−9092.
(28) Yoo, J.; Delaney, S.; Stemp, E. D. A.; Barton, J. K. *J. Am. Chem. Soc.* **2003**, *125*, 6640−6641.
(29) Fu, P. K. L.; Bradley, P. M.; van Loyen, D.; Heinz, D.; Bossmann, S. H.; Turro, C. *Inorg. Chem.* **2002**, *41*, 3808−3810.
(30) Duan, C-Y.; Lu, Z. L.; You, X-Z.; Zhou, Z-Y.; Mak, T. C. W.; Luo, Q.; Zhou, J-Y. *Polyhedron* **1998**, *17*, 4131−4138.

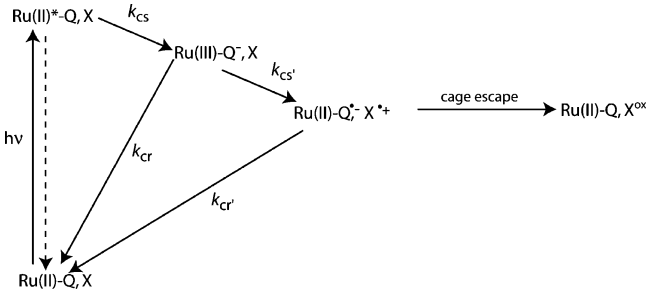

Figure 1. Modified flash-quench scheme for a covalently tethered Ru(II) quencher complex. Upon excitation with 450 nm light, the ruthenium(II) is raised to its excited state and is subsequently oxidized by the tethered quencher to form the powerful ground state oxidant, Ru(III). Ru(III) is capable of oxidizing DNA but can also recombine with the reduced quencher to reform the starting materials. X denotes a nucleotide base such as guanine which may be oxidized by Ru(III).

nium complexes in which a bipyridine ligand is covalently tethered to a quinone functionality.[31]

In the current study, we describe the synthesis and characterization of a ruthenium quencher conjugate, in which a ruthenium pentammine quencher is covalently tethered to a tris heteroleptic ruthenium complex via coordination to the imidazole of a bridging histidine. This system allows us to observe flash-quench-generated guanine damage, in addition to novel charge separation pathways. The spectroscopic results obtained illustrate the rich redox chemistry of ruthenium complexes interacting with DNA. Figure 1 shows this intramolecular flash-quench scheme.

Experimental Section

DNA Synthesis. DNA polymers were purchased from Amersham and dialyzed against a buffer of 10 mM sodium phosphate, 50 mM NaCl, pH 7.0, prior to use. Reagents for solid-phase DNA syntheses were purchased from Glen Research. Oligonucleotides with and without cyclopropylamine-modified bases were prepared on an Applied Biosytems 394 DNA synthesizer using standard phosphoramidite chemistry leaving the 5′-dimethoxytrityl group intact. Cyclopropylamine-containing strands were synthesized using the precursor bases 2-fluoroinosine and 4-thiouracil for N_2-cyclopropylcytosine (^{CP}G) and N_4-cyclopropylcytosine (^{CP}C) respectively. Cyclopropyl substitution was accomplished by incubating the resin in 1 M diaza(1,3)bicyclo[5.4.0]undecane (DBU) in acetonitrile for 2 h prior to overnight incubation in 6 M aqueous cyclopropylamine at 60 °C, resulting in simultaneous cleavage, deprotection, and substitution as indicated by MALDI-TOF mass spectrometry and analytical reversed-phase HPLC.[22] Oligonucleotides without cyclopropyl substitutions were cleaved from the resin and deprotected by incubation in NH_4OH overnight at 60 °C. Strands were purified by reversed-phase HPLC using a C18 column (Varian). The trityl group was removed by treatment with 80% acetic acid for 15 min, and the resulting strands were purified again by reversed-phase HPLC. All strands were characterized by MALDI-TOF mass spectrometry. Duplexes were annealed by heating equimolar amounts of complementary strands determined by absorbance at 260 nm to 90 °C and slow cooling to ambient temperature. Extinction coefficients for the strands are included in the Supporting Information.

Synthesis and Characterization of [Ru(phen)(dppz)(bpy′-his)]-Cl_2. All solid-phase reactions used dry solvents, which were purchased from Fluka and stored over molecular sieves. [Ru(phen)(dppz)(bpy′-his)]$^{2+}$ (bpy′-his = 4′ methyl-2,2′-bipyridine-4-butanoic acid (histidinyl)-amide, dppz = dipyrido[3,2-a:2′,3′-c]phenazine) (Figure 2) was prepared starting with [Ru(phen)(dppz)(bpy′)]$^{2+}$, the synthesis of which has been described.[32,33] Resin-bound Fmoc-His(Fmoc) was purchased from Bachem, and the Fmoc groups were removed with 20% piperidine in DMF prior to synthesis. The resin-bound histidine was combined with racemic [Ru(phen)(dppz)(bpy′)]$^{2+}$ (1 equiv), (benzotriazol-1-yloxy)tripyrrolidinophosphonium hexafluorophosphate (3 equiv), and diisopropylethylamine (6 equiv) in DMF, and the mixture was stirred at ambient temperature overnight in the dark. The complex was cleaved from the resin by being stirred with 95% aqueous TFA for 1 h; it was then precipitated by filtration into ice-cold *tert*-butyl methyl ether, washed with cold ether, and dried *in vacuo*. [Ru(phen)(dppz)(bpy′-his)]$^{2+}$ was purified by reversed-phase HPLC on a semipreparative Microsorb (Varian) C18 column using a water−acetonitrile (0.1% TFA) gradient and a flow rate of 4 mL min^{-1}. The percentage of acetonitrile was held constant at 15% for 15 min and then increased to 40% over 75 min. Chromatograms were monitored at 260, 370, and 450 nm with the desired isomer peaks eluting at 41 and 46 min.

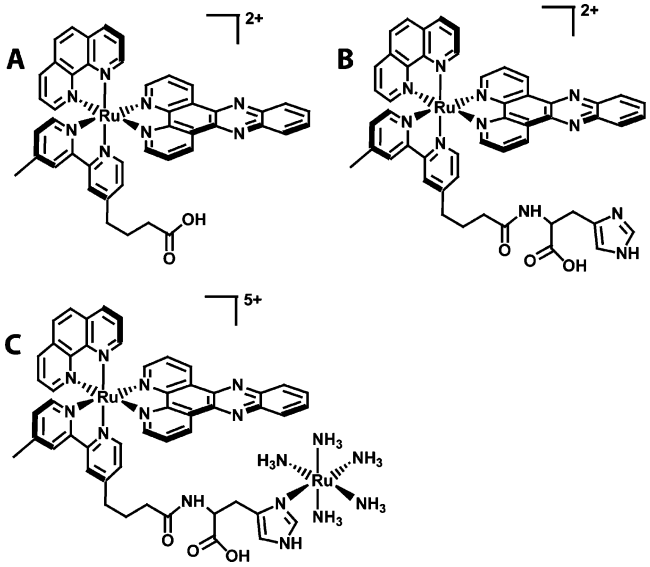

Figure 2. Tris heteroleptic dipyridophenazine complexes of ruthenium(II) used in the study. The parent complex, [Ru(phen)(dppz)(bpy′)]$^{2+}$ is shown in A; the histidine modified complex [Ru(phen)(dppz)(bpy′-his)]$^{2+}$ is shown in B, and the ruthenium pentammine-coordinated complex [{Ru(phen)(dppz)(bpy′-his)}{Ru(NH_3)$_5$}]$^{5+}$ is shown in C.

ESI and MALDI-TOF mass spectrometries were used to characterize [Ru(phen)(dppz)(bpy′-his)]$^{2+}$. Electrospray analyses were performed using a Perkin-Elmer/Sciex API 365 triple quadrupole tandem mass spectrometer, while MALDI analyses were performed on a PerSeptive Biosystems Voager Elite DE.str matrix-assisted laser desorption time-of-flight with delayed extraction and high sensitivity linear detector. ($C_{51}H_{41}N_{11}O_3Ru$ calcd: 478.1 (+2). Found: 478.5 (ESI)). ^{1}H NMR (600 MHz, CD_3CN): δ (aromatic Hs) 9.56 (m), 8.69 (d), 8.56 (m), 8.45 (m), 8.29 (m), 8.12 (m), 7.98 (d), 7.84 (m), 7.74 (m), 7.68 (m), 7.60 (m), 7.50 (m), 7.18 (m); (aliphatic Hs) 4.64 (d), 3.28 (d), 3.17 (m), 3.07 (d), 2.73 (s), 2.52 (s), 2.22 (s), 1.23 (m). The aromatic to aliphatic proton ratio is 23:12. Because the absorbance of histidine does not affect the

(31) Opperman, K. A.; Mecklenburg, S. L.; Meyer, T. J. *Inorg. Chem.* **1994**, *33*, 5295−5301.

(32) Strouse, G. F.; Anderson, P. A.; Schoonover, J. R.; Meyer, T. J.; Keene, F. R. *Inorg. Chem.* **1992**, *31*, 2618−2619.

(33) Anderson, P. A.; Deacon, G. B.; Haarman, K. H.; Keene, F. R.; Meyer, T. J.; Reitsma, D. A.; Skelton, B. W.; Strouse, G. F.; Thomas, N. C.; Treadway, J. A.; White, A. H. *Inorg. Chem.* **1995**, *34*, 6145−6157.

440 nm MLCT transition of ruthenium complexes, [Ru(phen)(dppz)(bpy′-his)]$^{2+}$ was confirmed to have the same extinction coefficient as [Ru(phen)(dppz)(bpy′)]$^{2+}$ of 19 500 M^{-1} cm^{-1} at 440 nm, as shown by ICP−MS.

Synthesis and Characterization of [{Ru(phen)(dppz)(bpy′-his)}{Ru(NH$_3$)$_5$}]Cl$_5$. [{Ru(phen)(dppz)(bpy′-his)}{Ru(NH$_3$)$_5$}]$^{5+}$ (Figure 2) was synthesized in a manner similar to that for [Ru(phen)(dppz)(bpy′-his)]$^{2+}$, as described above with one additional step. After the coupling with [Ru(phen)(dppz)(bpy′)]$^{2+}$, the reddish-orange resin was reacted with chloropentammineruthenium(III) chloride by procedures established to prepare ruthenium-modified proteins.[25] The [Ru(phen)(dppz)(bpy′)]$^{2+}$-tethered histidine-bound resin was stirred for 1.5 days under argon in aqueous 50 mM [Ru(NH$_3$)$_5$(H$_2$O)]$^{2+}$ prepared from the reduction of [Ru(NH$_3$)$_5$Cl]$^{2+}$ (Strem) with zinc amalgam.[34,35] After coordination of [Ru(NH$_3$)$_5$(H$_2$O)]$^{2+}$, generated in situ, to histidine, the complex was exposed to air for 6 h to promote oxidation of the coordinated quencher moiety. The complex was then cleaved from the resin following the same procedure as described above for [Ru(phen)(dppz)(bpy′-his)]$^{2+}$. HPLC analysis following precipitation and lyophilization showed the presence of two isomers. These eluted at 39 and 43 min using the same gradient as described above for the purification of [Ru(phen)(dppz)(bpy′-his)]$^{2+}$.

MALDI-TOF mass spectrometric analysis of [{Ru(phen)(dppz)(bpy′-his)}{Ru(NH$_3$)$_5$}]$^{5+}$ showed mainly a product with the same mass and isotopic distribution as [Ru(phen)(dppz)(bpy′-his)]$^{2+}$. However, ESI shows a small peak corresponding to the 3+ ion of [{Ru(phen)(dppz)(bpy′-his)}{Ru(NH$_3$)$_5$}] ($C_{51}H_{54}N_{16}O_3Ru_2$ calcd 380.75; found 380.0). The mass distribution for this 3+ ion matches the simulated mass spectrum (see Supporting Information). HPLC analysis after irradiation with a 442 nm laser indicated decomposition to the [Ru(phen)(dppz)(bpy′-his)]$^{2+}$ complex (vide infra). The ruthenium content of equimolar solutions of [Ru(phen)(dppz)(bpy′-his)]$^{2+}$ and [{Ru(phen)(dppz)(bpy′-his)}{Ru(NH$_3$)$_5$}]$^{5+}$ was measured by ICP−MS and [{Ru(phen)(dppz)(bpy′-his)}{Ru(NH$_3$)$_5$}]$^{5+}$ was found to contain twice the ruthenium content of [Ru(phen)(dppz)(bpy′-his)]$^{2+}$. The predicted ruthenium ratio for [Ru(phen)(dppz)(bpy′-his)]$^{2+}$/[{Ru(phen)(dppz)(bpy′-his)}{Ru(NH$_3$)$_5$}]$^{5+}$ = 1:2 (found = 1:1.95).

Steady-State Fluorescence. Steady-state emission spectra of the ruthenium complexes were recorded at ambient temperature using an ISS K2 spectrofluorimeter in a 5 mm path length cell. Ruthenium-containing samples (prepared to have an absorbance of 0.15 at 440 nm in either acetonitrile or buffer of 10 mM sodium phosphate, 50 mM NaCl, pH 7 with 1 mM poly d(AT) or poly d(GC)) were excited at 440 nm, and the emission was recorded over a wavelength range of 500−800 nm.

Electrochemistry. Ground state oxidation and reduction potentials for [{Ru(phen)(dppz)(bpy′-his)}{Ru(NH$_3$)$_5$}]$^{5+}$, [Ru(phen)(dppz)(bpy′-his)]$^{2+}$, and [Ru(phen)(dppz)(bpy)]$^{2+}$ were obtained under an argon atmosphere using a CH Instruments Electrochemical Workstation Analyzer. A glassy carbon working electrode, Ag/AgCl reference electrode, and Pt auxiliary electrode were used in a single-cell sample apparatus. Ferrocence carboxylic acid ($E_{1/2}$ = 0.33 V vs Ag/AgCl) was used as an external reference. Samples were prepared for oxidation measurements in dry acetonitrile, while those for reduction measurements were prepared in dry DMF. All solutions contained 100 mM tetrabutylammonium hexafluorophosphate as the supporting electrolyte and were degassed by bubbling argon through the sample prior to the reading. Metal concentrations for electrochemical analysis ranged from 0.1 to 0.5 mM. Experiments were performed in the dark. Values reported in volts versus NHE.

Assay for DNA Oxidation. DNA strands were labeled at the 5′ end with [^{32}P] γ-ATP using polynucleotide kinase[36] and purified on a 20% denaturing polyacrylamide gel (Sequagel). The desired band was identified by autoradiography, excised from the gel, and eluted into 500 mM NH_4OAc. Labeled DNA was isolated using Micro Bio-Spin 6 columns (BioRad) and hybridized to the complementary strand in 10 mM sodium phosphate, 50 mM sodium chloride, pH 7.0. Aliquots (30 μL) of 4 μM duplex were incubated with equimolar ruthenium complex and 80 μM [Ru(NH$_3$)$_6$]$^{3+}$ quencher (if added externally) and irradiated at 442 nm for 30 min using a Liconix He:Cd laser (~12 mW at 442 nm). After irradiation, samples were treated with 10% piperidine, heated to 90 °C for 30 min, and dried *in vacuo*. Samples were electrophoresed on 20% denaturing polyacrylamide gels for 1.5 h at 90 W and imaged using a Storm 820 phosphoimager (Molecular Dynamics/ GE Healthcare). Oxidative damage products were quantified by phosphoimagery using Image Quant 5.2 (Molecular Dynamics).

Analysis of ^{CP}G/^{CP}C Ring Opening. Experiments were performed using analogous methods as described in ref 20. Ruthenium-containing samples (5 μM metal, 5 μM duplex, and 50 μM [Ru(NH$_3$)$_6$]$^{3+}$ quencher (if used) in 30 μL of 10 mM sodium phosphate, 50 mM NaCl, pH 7.0) were prepared using the freeze−pump−thaw method and were stored under argon in airtight cuvettes (NMR tubes welded onto a Teflon gastight top (J. Young, Scientific Glassware)). Samples were irradiated on a Liconix 442 nm He:Cd laser (~12 mW) for various time increments between 5 and 60 min.[20] Light controls (DNA, no metal) at 30 and 60 min were obtained. After irradiation, the duplexes were digested into deoxynucleosides by overnight incubation at 37 °C with alkaline phosphatase (Roche), phosphodiesterase I (USB), and S1 nuclease (Amersham Biosciences). Once the digestion was complete, the samples were diluted with water and analyzed by reversed-phase HPLC using a Chemcobond 5-ODS C18 column. Deoxynucleosides eluted between 7 and 18 min using a gradient of 2−14% MeCN against 50 mM NH_4OAc over 30 min. The cyclopropylguanine deoxynucleoside eluted at 25 min, and the ring-opened product, hydroxypropylguanine, eluted at 19 min; the cyclopropylcytosine deoxynucleoside eluted at 19 min.

EPR Spectroscopy. EPR spectra were recorded at 20 K using an X-band Bruker EMX spectrometer equipped with a standard rectangular TE102 cavity. Experiments were conducted with an Oxford (ES9000) continuous-flow helium cryostat (temperature range = 3.6−300 K). Frequency values were accurately measured using a frequency counter built into the microwave bridge. Samples were irradiated in standard EPR quartz tubes while simultaneously freezing in an unsilvered Dewar filled with liquid nitrogen.[37] The light source was a 300 W Xe-arc lamp (Varian, Eimac division, Light R300-3), powered by an illuminator power supply (Varian, Eimac division, model PS 300-1). UV filters were employed to eliminate light <320 nm. Samples contained 0.1 mM [{Ru(phen)(dppz)(bpy′-his)}{Ru(NH$_3$)$_5$}]$^{5+}$ and 1.5 mM base pairs of DNA polymer in 10 mM sodium phosphate, 50 mM NaCl, pH 7.0. EPR parameters were as follows: receiver gain, 5.64 × 10^3; modulation amplitude, 4 G; and microwave power, 1.27 mW.

(34) Sundberg, R. J.; Gupta, G. *Bioinorg. Chem.* **1973**, *3*, 39−48.
(35) Yocom, K. Ph.D. Thesis, California Institute of Technology, LOCATION, 1982.
(36) Sambrook, J.; Fritsch, E. D.; Maniatis, T. *Molecular Cloning: A Laboratory Manual*, 2nd ed.; Cold Spring Harbor Laboratory: New York, 1989.
(37) The characteristics of the guanine radical signal detected here in aqueous buffers are comparable to that found earlier using a glycerol-based cryoprotectant.

Laser Spectroscopy. Time-resolved emission and transient absorption measurements were recorded using a frequency-doubled Nd:YAG-pumped OPO laser for excitation of the ruthenium lumiphore ($\lambda_{ex} = 480$ nm).[24] A pulsed 75 W Xe-arc lamp (Photon Technology International) was used as the probe source for the transient absorption measurements. Individual data sets were the average of 1000 shots. Data were collected using an oscilloscope (LeCroy) and transferred to a computer using Scope Explorer 2.19 (LeCroy). Data fitting was accomplished using a nonlinear least-squares analysis in Origin 6.1 (Microcal). Difference spectra were generated by subtraction of the average of pretrigger absorbances from an average of posttrigger absorbances at a particular time point. Unless otherwise specified, difference spectra were measured using 30 μM metal complex, 1 mM base pairs of polymer in 10 mM sodium phosphate, 50 mM NaCl, pH 7.0.

Experiments at low pH were carried out using 10 mM sodium acetate, 50 mM NaCl, pH 5, and experiments investigating the effect of Zn^{2+} were carried out using 2.5 mM $ZnCl_2$, 10 mM sodium phosphate, 50 mM NaCl, pH 7.0. Samples were measured in a stirring cuvette (Starna) and were continuously stirred during the acquisition. Experiments using $[Ru(NH_3)_5(H_2O)]^{2+}$ were carried out in an airtight stirring cuvette (Starna) with a fused top connected to an additional freeze−pump−thaw chamber. $[Ru(NH_3)_5(H_2O)]^{2+}$ was generated by mixing $[Ru(NH_3)_5Cl]Cl_2$ with zinc amalgam until it reduced and solubilized. The reduced $[Ru(NH_3)_5(H_2O)]^{2+}$ was then combined with a $[Ru(phen)(dppz)(bpy'\text{-}his)]^{2+}$, poly-d(AT) solution in 10 mM sodium phosphate, 50 mM NaCl, pH 7 that had been degassed using the freeze−pump−thaw technique. The final sample concentration was 0.3 mM $[Ru(NH_3)_5(H_2O)]^{2+}$ and 30 μM $[Ru(phen)(dppz)(bpy'\text{-}his)]^{2+}$ in 1 mM poly-d(AT). Single-wavelength measurements were obtained using 30 μM complex, 1 mM base pairs of polymer, in the same buffer.

Results and Discussion

Experimental Design. The properties and DNA interactions of a novel tris heteroleptic ruthenium complex with a tethered ruthenium pentammine quencher moiety have been examined. Dppz-containing ruthenium(II) polypyridyl complexes in the presence of oxidative quenchers can generate the powerful ground state oxidant, Ru(III), which is capable of oxidizing guanine-containing DNA. However, the formation of the guanine radical is limited by the rate of production of Ru(III), which in turn is limited by the rate of diffusional quenching of the Ru(II) excited state. As shown in Figure 1, direct attachment of the quencher to the bipyridine ligand via a bridging histidine circumvents the rate-limiting step of diffusional quenching in traditional flash-quench methodologies. Here we compare the properties of the tethered quencher complex, $[\{Ru(phen)(dppz)(bpy'\text{-}his)\}\{Ru(NH_3)_5\}]^{5+}$, with the parent complex, $[Ru(phen)(dppz)(bpy')]^{2+}$, and the histidine-modified complex without quencher, $[Ru(phen)(dppz)(bpy'\text{-}his)]^{2+}$ (Figure 2).

Synthesis and Characterization of $[\{Ru(phen)(dppz)(bpy'\text{-}his)\}\{Ru(NH_3)_5\}]^{5+}$ and $[Ru(phen)(dppz)(bpy'\text{-}his)]^{2+}$. Solid-phase peptide chemistry was used to couple histidine to the carboxylic acid-functionalized $[Ru(phen)(dppz)(bpy')]^{2+}$, resulting in the formation of $[Ru(phen)(dppz)(bpy'\text{-}his)]^{2+}$ (Figure 3). Further reaction with reduced ruthenium pentammine afforded $[\{Ru(phen)(dppz)(bpy'\text{-}his)\}\{Ru(NH_3)_5\}]^{5+}$. The complexes were synthesized in low yield, ranging from 1 to 5% $[\{Ru(phen)(dppz)(bpy'\text{-}his)\}\{Ru(NH_3)_5\}]^{5+}$ and 15−30% $[Ru(phen)(dppz)(bpy'\text{-}his)]^{2+}$. The identity of $[Ru(phen)(dppz)(bpy'\text{-}his)]^{2+}$ was confirmed by ESI and MALDI-TOF mass spectrometries, while the resulting coordination of the additional ruthenium moiety on $[\{Ru(phen)(dppz)(bpy'\text{-}his)\}\{Ru(NH_3)_5\}]^{5+}$ was confirmed by ICP−MS. ESI also showed the correct mass of the 3+ ion.[38]

Because there are four isomers of the starting $[Ru(phen)(dppz)(bpy')]^{2+}$, $[Ru(phen)(dppz)(bpy'\text{-}his)]^{2+}$ and $[\{Ru(phen)(dppz)(bpy'\text{-}his)\}\{Ru(NH_3)_5\}]^{5+}$ also consist of four diastereomers; either a Λ or Δ configuration at the metal center, and either an axial or equatorial disposition of the functionalized bpy.[38] Of these four isomers, only the axial versus equatorial forms were resolvable by HPLC analysis as two distinct peaks. Both peaks were collected and combined for subsequent experiments. The two isomer peaks of $[\{Ru(phen)(dppz)(bpy'\text{-}his)\}\{Ru(NH_3)_5\}]^{5+}$ are shifted by ~1 min from those of $[Ru(phen)(dppz)(bpy'\text{-}his)]^{2+}$, which are in turn shifted by ~1 min from those of the starting complex, $[Ru(phen)(dppz)(bpy')]^{2+}$ (see Supporting Information).

The $[\{Ru(phen)(dppz)(bpy'\text{-}his)\}\{Ru(NH_3)_5\}]^{5+}$ complex is unstable under conditions of constant irradiation at 442 nm as evidenced by a loss of emission quenching and the corresponding return of luminescence, as well as a shift in HPLC retention time (see Supporting Information). The emission intensity of $[\{Ru(phen)(dppz)(bpy'\text{-}his)\}\{Ru(NH_3)_5\}]^{5+}$ in poly-d(AT) and in acetonitrile was measured prior to irradiation at 442 nm. After 60 min of irradiation, the intensity of $[\{Ru(phen)(dppz)(bpy'\text{-}his)\}\{Ru(NH_3)_5\}]^{5+}$ in both samples increases dramatically but is more pronounced in acetonitrile. The irradiated samples were then subjected to HPLC analysis which revealed decomposition of the complex to $[Ru(phen)(dppz)(bpy'\text{-}his)]^{2+}$. All experiments described below were performed under conditions in which the complex was stable and not subject to constant irradiation.

Steady-State Luminescence. Upon excitation into the metal-to-ligand charge transfer (MLCT) band, dppz complexes of Ru(II) are highly emissive when intercalated into DNA but show significant quenching when measured in aqueous buffer because of hydrogen bonding to the phenazine nitrogen atoms.[39,40] Thus, these complexes exhibit a "light-switch" effect in DNA because intercalation of the dppz ligand into the DNA π-stack protects the phenazine nitrogens from quenching by aqueous solvent, restoring luminescence. To determine if the novel complexes exhibit light-switch behavior, we measured their luminescence properties in organic solvent and DNA. The steady-state quantum yields of $[Ru(phen)(dppz)(bpy'\text{-}his)]^{2+}$ and $[\{Ru(phen)(dppz)(bpy'\text{-}his)\}\{Ru(NH_3)_5\}]^{5+}$ relative to $[Ru(bpy)_3]^{2+}$ measured in

(38) Copeland, K. D.; Lueras, A. M.; Stemp, E. D. A.; Barton, J. K. *Biochemistry* **2002**, *41*, 12785−12797.
(39) Olson, E. J. C.; Hu, D.; Hormann, A.; Jonkman, A. M.; Arkin, M. R.; Stemp, E. D. A.; Barton, J. K.; Barbara, P. F. *J. Am. Chem. Soc.* **1997**, *119*, 11458−11467.
(40) Friedman, A. E.; Chambron, J. C.; Sauvage, J. P.; Turro, N. J.; Barton, J. K. *J. Am. Chem. Soc.* **1990**, *112*, 4960−4961.

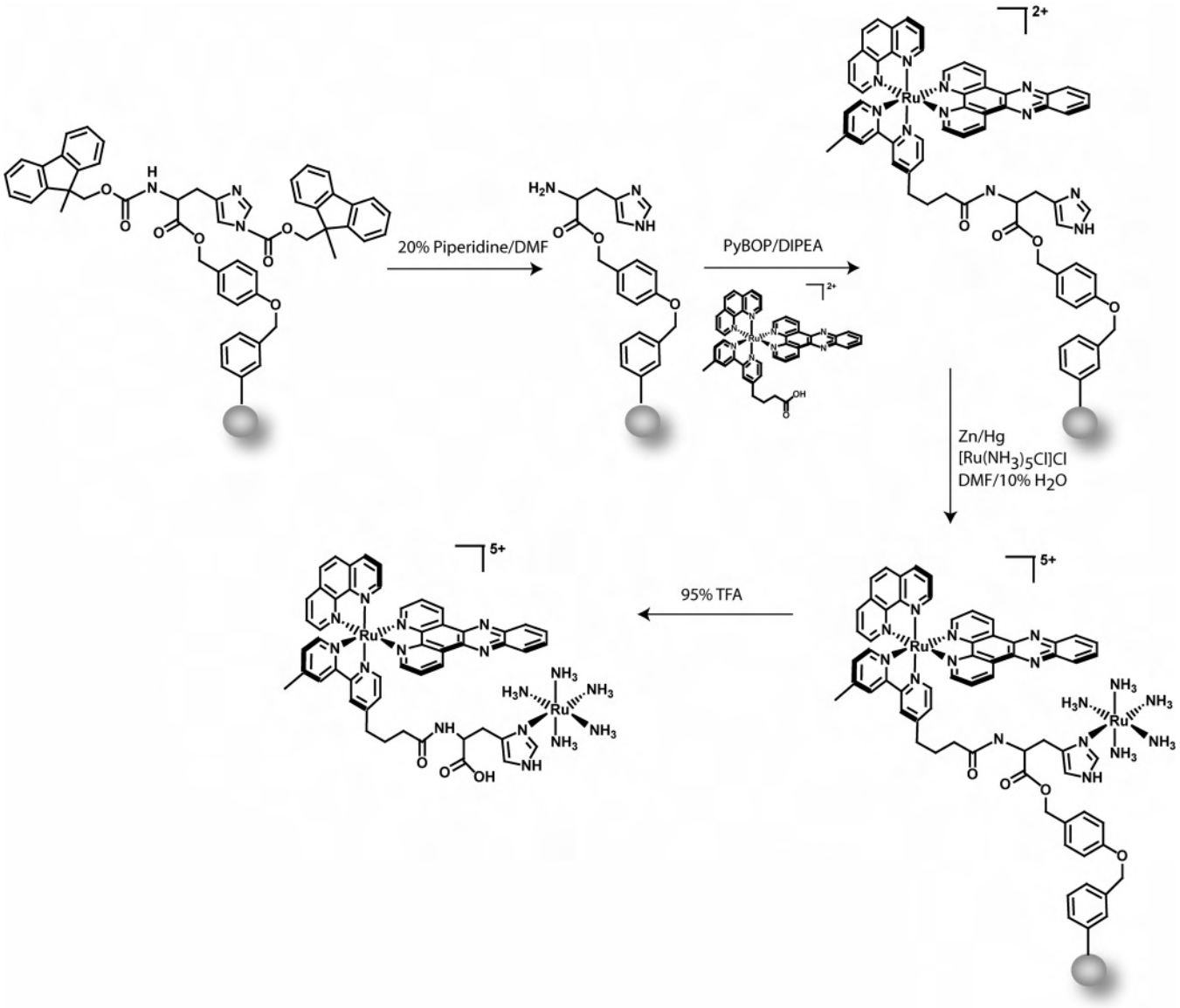

Figure 3. Scheme for generating $[Ru(phen)(dppz)(bpy'\text{-}his)]^{2+}$ and $[\{Ru(phen)(dppz)(bpy'\text{-}his)\}\{Ru(NH_3)_5\}]^{5+}$using solid-phase peptide chemistry. Fmoc-His(Fmoc) is deprotected with piperidine and reacted with $[Ru(phen)(dppz)(bpy')]^{2+}$. This can be cleaved from the resin with TFA to yield $[Ru(phen)(dppz)(bpy'\text{-}his)]^{2+}$ or further reacted with $[Ru(NH_3)_5Cl]Cl_2$ to form $[\{Ru(phen)(dppz)(bpy'\text{-}his)\}\{Ru(NH_3)_5\}]^{5+}$.

acetonitrile and the DNA polymers poly-d(AT) and poly-d(GC) are shown in Table 1. Similar to $[Ru(phen)(dppz)(bpy')]^{2+}$ and related dipyridophenazine complexes of ruthenium(II), $[Ru(phen)(dppz)(bpy'\text{-}his)]^{2+}$ and $[\{Ru(phen)(dppz)(bpy'\text{-}his)\}\{Ru(NH_3)_5\}]^{5+}$ are non-emissive in water. These complexes also luminesce in acetonitrile, providing a comparison for DNA-specific characteristics. $[Ru(phen)(dppz)(bpy'\text{-}his)]^{2+}$ and $[Ru(phen)(dppz)(bpy')]^{2+}$ show substantial luminescence in acetonitrile, poly-d(GC), and poly-d(AT). $[\{Ru(phen)(dppz)(bpy'\text{-}his)\}\{Ru(NH_3)_5\}]^{5+}$, however, is quenched under all three environments, and its emission is comparable to that of $[Ru(phen)(dppz)(bpy'\text{-}his)]^{2+}$ and $[Ru(phen)(dppz)(bpy')]^{2+}$ with a large excess of added $[Ru(NH_3)_6]^{3+}$ quencher. All three complexes show luminescence only when bound to DNA polymers, with intensities being slightly higher in poly-d(AT) than in poly-d(GC). This luminescence enhancement, along with a hypochromism in the dppz band (data not shown), is consistent with intercalative binding. It should also be noted that the maximum wavelength for emission is blue-shifted upon binding to the GC polymer (620 nm) relative to the AT polymer or in acetonitrile (630 nm), consistent with previously published results for $[Ru(phen)_2(dppz)]^{2+}$ and $[Ru(bpy)_2(dppz)]^{2+}$.[41]

Time-Resolved Emission. Steady-state luminescence measurements indicate that $[\{Ru(phen)(dppz)(bpy'\text{-}his)\}\{Ru(NH_3)_5\}]^{5+}$ is substantially quenched in acetonitrile and when intercalated in DNA, relative to the parent complexes. To probe this chemistry further, we compared the excited state lifetimes of $[\{Ru(phen)(dppz)(bpy'\text{-}his)\}\{Ru(NH_3)_5\}]^{5+}$ to those of the parent complexes in the two DNA polymers, poly-d(AT) and poly-d(GC). The excited state of the intercalated dppz complexes of ruthenium(II) decays with two lifetimes in the presence of DNA, reflecting two different

(41) Jenkins, Y.; Friedman, A. E.; Turro, N. J.; Barton, J. K. *Biochemistry* **1992**, *31*, 10809−10816.

Table 1. Steady-State Luminescence Quantum Yields[a]

complex[b]	MeCN	poly-d(GC)[c]	poly-d(AT)[c]
[{Ru(phen)(dppz)(bpy′-his)}{Ru(NH$_3$)$_5$}]$^{5+}$	0.10	0.15	0.12
[Ru(phen)(dppz)(bpy′-his)]$^{2+}$	0.84	0.43	0.32
[Ru(phen)(dppz)(bpy′-his)]$^{2+}$ + Q[d]		0.16	0.10
[Ru(phen)(dppz)(bpy′)]$^{2+}$	0.99	0.44	0.34
[Ru(phen)(dppz)(bpy′)]$^{2+}$ + Q		0.15	0.11

[a] Relative to [Ru(bpy)$_3$]$^{2+}$ in MeCN with excitation at 440 nm. Errors are less than 6%. [b] Complexes were measured to have an absorbance of 0.15 at 440 nm. [c] Measured at 20 °C in 1 mM nucleotides in 10 mM sodium phosphate, 50 mM NaCl, pH 7 [d] Q = [Ru(NH$_3$)$_6$]$^{3+}$ added in a 10-fold excess to that of the Ru(II) complex

Table 2. Ru(II)* Excited State Lifetimes[a]

	poly-d(GC)[c]		poly-d(AT)[c]	
complex[b]	τ_1, ns (%)	τ_2, ns (%)	τ_3, ns (%)	τ_4, ns (%)
[{Ru(phen)(dppz)(bpy′-his)}{Ru(NH$_3$)$_5$}]$^{5+}$	56 (40)	17 (60)	154 (11)	33 (89)
[{Ru(phen)(dppz)(bpy′-his)}{Ru(NH$_3$)$_5$}]$^{5+}$ + Q[d]	61 (10)	19 (90)		20 (100)
[Ru(phen)(dppz)(bpy′-his)]$^{2+}$	203 (38)	53 (62)	192 (42)	54 (58)
[Ru(phen)(dppz)(bpy′-his)]$^{2+}$ +Q	49 (9)	16 (91)	167 (3)	21 (97)

[a] Measured at 610 nm, excitation λ = 480 nm. Data were fit to $y(t) = 100[C1\exp^{(-t/\tau1)}+(1 - C1)\exp^{(-t/\tau2)}]$ by a nonlinear least-squares method with convolution of the instrument response function using Origin 6.1 as described previously. Errors are ±10%. See ref 58. [b] Measured in 1 mM nucleotides, 10 mM sodium phosphate, 50 mM NaCl, pH 7. [c] Complex concentrations were 30 μM. [d] Q = [Ru(NH$_3$)$_6$]$^{3+}$

binding modes.[42] These binding modes have been proposed to arise from the position of the phenazine−metal axis with respect to that of the DNA base pair; the longer lifetime component is assigned to a binding mode in which the intercalated dppz ligand stacks between the bases from the major groove with the metal−phenazine axis perpendicular to the base pair long axis, protecting both phenazine nitrogens, while the shorter lifetime is assigned to the "side-on" binding mode, where one of the phenazine nitrogens is more exposed to solvent quenching.[43]

Time-resolved measurements show a biexponential decay of emission for [Ru(phen)(dppz)(bpy′-his)]$^{2+}$ and [{Ru(phen)(dppz)(bpy′-his)}{Ru(NH$_3$)$_5$}]$^{5+}$ in the presence of DNA consistent with two binding modes for the complexes (Table 2). In the absence of DNA, the excited complex decays with one lifetime. Consistent with the steady state emission intensities, both excited state lifetimes in [{Ru(phen)(dppz)(bpy′-his)}{Ru(NH$_3$)$_5$}]$^{5+}$ are reduced when compared with those of [Ru(phen)(dppz)(bpy′-his)]$^{2+}$. The [Ru(phen)(dppz)(bpy′-his)]$^{2+}$ and [{Ru(phen)(dppz)(bpy′-his)}{Ru(NH$_3$)$_5$}]$^{5+}$ excited states decays are distributed evenly between the shorter and longer lifetimes in poly-d(AT). However, in poly-d(GC), the majority of [{Ru(phen)(dppz)(bpy′-his)}{Ru(NH$_3$)$_5$}]$^{5+}$ decays with the shorter lifetime. The addition of the external quencher, [Ru(NH$_3$)$_6$]$^{3+}$ results in a shortening of both excited state lifetimes in [Ru(phen)(dppz)(bpy′-his)]$^{2+}$. This quenching is not seen in [{Ru(phen)(dppz)(bpy′-his)}{Ru(NH$_3$)$_5$}]$^{5+}$, where the addition of external quencher has negligible effects on the emission lifetimes because the emission is already substantially quenched. As can be seen in Table 2, the lifetimes of the complex bound to poly-d(AT) are slightly longer than when bound to poly-d(GC), likely reflecting different intercalative binding modes of the complex to each polymer. Indeed, previous results have shown shorter lifetimes for ruthenium complexes bound to the GC polymer, presumably because of more solvent accessibility when bound to the GC rich sequence.[44] This is, however, a small effect since, if a weighted average lifetime is calculated, there is little difference between the decay in the AT and GC polymers for all of the complexes listed in Table 2.

Electrochemistry of Ruthenium Complexes. As shown in Figure 4 and Table 3, the three complexes [Ru(phen)(dppz)(bpy)]$^{2+}$, [Ru(phen)(dppz)(bpy′-his)]$^{2+}$, and [{Ru(phen)(dppz)(bpy′-his)}{Ru(NH$_3$)$_5$}]$^{5+}$ show electrochemical profiles with similar oxidation and reduction potentials. The oxidation profiles for [Ru(phen)(dppz)(bpy)]$^{2+}$ and [Ru(phen)(dppz)(bpy′-his)]$^{2+}$ reveal a single peak at ∼1.5 V vs NHE (see Supporting Information). The reduction profile shows three waves occurring between −0.68 and −1.55 V vs NHE, consistent with reduction of each ligand. [Ru(phen)(dppz)(bpy)]$^{2+}$ shows large reversible reduction waves, while [Ru(phen)(dppz)(bpy′-his)]$^{2+}$ exhibits weaker reduction waves which are only quasi-reversible. Covalent attachment of the quencher moiety to [Ru(phen)(dppz)(bpy′-his)]$^{2+}$ restores the large reversible reduction waves. The relative intensities of the reduction peaks are different for [Ru(phen)(dppz)(bpy)]$^{2+}$ and [Ru(phen)(dppz)(bpy′-his)]$^{2+}$ as compared to [{Ru(phen)(dppz)(bpy′-his)}{Ru(NH$_3$)$_5$}]$^{5+}$. For [Ru(phen)(dppz)(bpy′)]$^{2+}$ and [Ru(phen)(dppz)(bpy′-his)]$^{2+}$, the reductions at ∼ −1.5 and −1.05 V vs NHE are larger than the reduction at −0.7 V vs NHE. However, the first reduction peak at −0.7 V vs NHE is larger than the other reductions in [{Ru(phen)(dppz)(bpy′-his)}{Ru(NH$_3$)$_5$}]$^{5+}$.

Photooxidation Experiments. Permanently damaged oxidative DNA products resulting from the flash-quench technique are often detectable by gel electrophoresis as piperidine-labile products of guanine oxidation.[12,19] Using a ^{32}P 5′-end-labeled sequence containing two sets of double guanine sites, we determined flash-quench generated oxidative damage for the three complexes with and without external [Ru(NH$_3$)$_6$]$^{3+}$quencher (Figure 5). Considerable 5′-specific guanine damage is observed for all three complexes in the presence of quencher. This 5′-specific damage pattern is not observed for any of the complexes alone, consistent with previous reports in which permanent flash-quench generated oxidative damage requires both light and quencher.[19,24]

It is initially surprising that [{Ru(phen)(dppz)(bpy′-his)}{Ru(NH$_3$)$_5$}]$^{5+}$, being significantly quenched spectroscopically, does not generate permanently oxidized guanine products. However, because the neutral guanine radical reacts on the millisecond time scale with water to form permanently

(42) Hartshorn, R. M.; Barton, J. K. *J. Am. Chem. Soc*. **1992**, *114*, 5919−5925.
(43) Dupureur, C. M.; Barton, J. K. *Inorg. Chem.* **1997**, *36*, 33−43.
(44) Stemp, E. D. A.; Holmlin, R. E.; Barton, J. K. *Inorg. Chim. Acta* **2000**, *297*, 88−97.

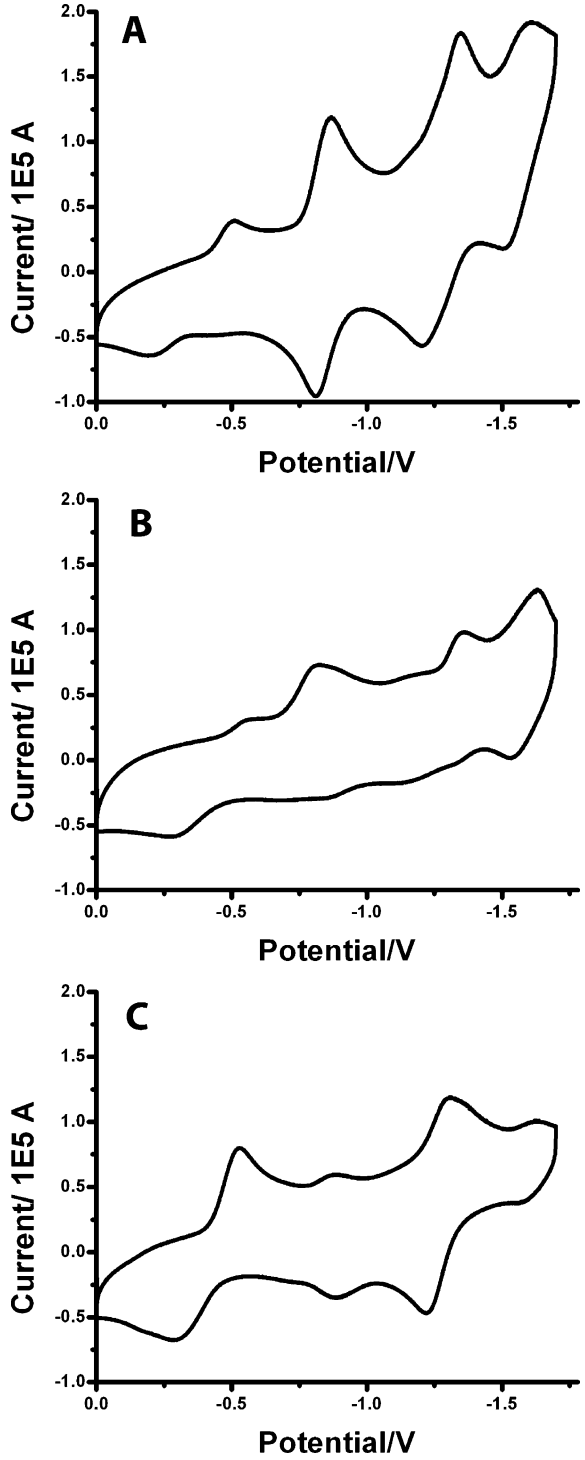

Figure 4. Electrochemistry of ruthenium complexes. Shown are cyclic voltammograms for reduction of $[\{Ru(phen)(dppz)(bpy'\text{-}his)\}\{Ru(NH_3)_5\}]^{5+}$ (A), $[Ru(phen)(dppz)(bpy'\text{-}his)]^{2+}$ (B), and $[Ru(phen)(dppz)(bpy)]^{2+}$ (C) measured in dry DMF with 0.1 M tetrabutylammonium hexafluorophosphate. Values reported in V vs NHE. See Experimental Section.

damaged products,[12] it is likely that fast back electron transfer either between Ru(III) and the reduced quencher or between the guanine radical and Ru(III) competes with this process, thereby preventing formation of permanent guanine oxidation products. Thus we sought to find a method in which guanine oxidation could be observed on a faster time scale. In the cyclopropylamine-modified nucleoside system originally developed by Saito,[45] oxidative ring opening occurs on a subnanosecond to picosecond time scale.[23] A similar sequence to that used in the gel electrophoresis experiments was modified to contain a cyclopropyl-modified guanine at the 5′ of the second double guanine set (Figure 6). We investigated ^{CP}G and ^{CP}C ring opening using our ruthenium complexes in two duplexes, G-2 and C-1 containing ^{CP}G and ^{CP}C, respectively. Since singlet oxygen is generated upon photolysis of the ruthenium complex in the absence of quencher,[46,47] and singlet oxygen can potentially contribute to ring opening, all ruthenium samples were irradiated under anaerobic conditions. When oxygen is eliminated from the system, damage patterns resulting from charge transfer events are revealed. It should be noted that in the presence of oxygen, ^{CP}C and ^{CP}G ring opening is observed with and without $[Ru(NH_3)_6]^{3+}$ quencher, although the effect is more pronounced in the case of ^{CP}G.[20] Under anaerobic conditions, ensuring ring opening is not the result of singlet oxygen sensitization, ^{CP}G decomposition was measured as a function of irradiation time (Figure 6). Light controls composed of DNA without any metal complex do not show cyclopropyl nucleoside decomposition (data not shown). Additionally, $[Ru(phen)(dppz)(bpy'\text{-}his)]^{2+}$ and $[Ru(phen)(dppz)(bpy')]^{2+}$ do not facilitate cyclopropyl ring opening without added quencher. When quencher is added to these complexes, however, rapid decomposition of the ^{CP}G nucleoside is observed. Importantly, irradiation of $[\{Ru(phen)(dppz)(bpy'\text{-}his)\}\{Ru(NH_3)_5\}]^{5+}$ is able to promote complete decomposition of ^{CP}G after 60 min without added quencher. This result is consistent with fast back electron transfer in the complex contributing to the lack of guanine damage detected by gel electrophoresis. It should be noted that an alternate explanation for the oxidation of the ^{CP}G nucleoside could arise from decomposition of the quencher-bound ruthenium complex over time to yield the parent ruthenium complex and a dissociated quencher. However, this is unlikely as the concentration of the dissociated quencher, if it were to become oxidized, would be far less than the concentration needed to effect damage because the concentration of the exogenous added quencher is in great excess of the metallointercalator. Additionally, the $[Ru(NH_3)_5(H_2O)]^{2+}$ species likely formed upon decomposition would preferentially coordinate with DNA rather than react by redox chemistry.[48]

Table 3. Electrochemical Potentials for Ruthenium Complexes[a]

complex	$E°$ $(3^+/2^+)$[b]	$E_{1/2}$[c] 1	2	3
$[Ru(phen)(dppz)(bpy)]^{2+}$	1.5	−0.7	−1.0	−1.5
$[Ru(phen)(dppz)(bpy'\text{-}his)]^{2+}$	1.5	−0.7	−1.0	−1.5
$[\{Ru(phen)(dppz)(bpy'\text{-}his)\}\{Ru(NH_3)_5\}]^{5+}$		−0.7	−1.1	−1.5

[a] Values reported in V vs NHE. [b] Measured in dry MeCN with 0.1 M tetrabutylammonium hexafluorophosphate. [c] Measured in dry DMF with 0.1 M tetrabutylammonium hexafluorophosphate.

(45) Nakatani, K.; Dohno, C.; Saito, I. *J. Am. Chem. Soc*. **2001**, *123*, 9861−9862.
(46) Mei, H.-Y.; Barton, J. K. *J. Am. Chem. Soc*. **1986**, *108*, 7414−7416.
(47) Mei, H.-Y.; Barton, J. K. *Proc. Natl. Acad. Sci. U.S.A.* **1988**, *85*, 1339−1343.
(48) Clarke, M. J.; Jansen, B.; Marx, K. A.; Kruger, R. *Inorg. Chim. Acta*. **1986**, *124*, 13−28.

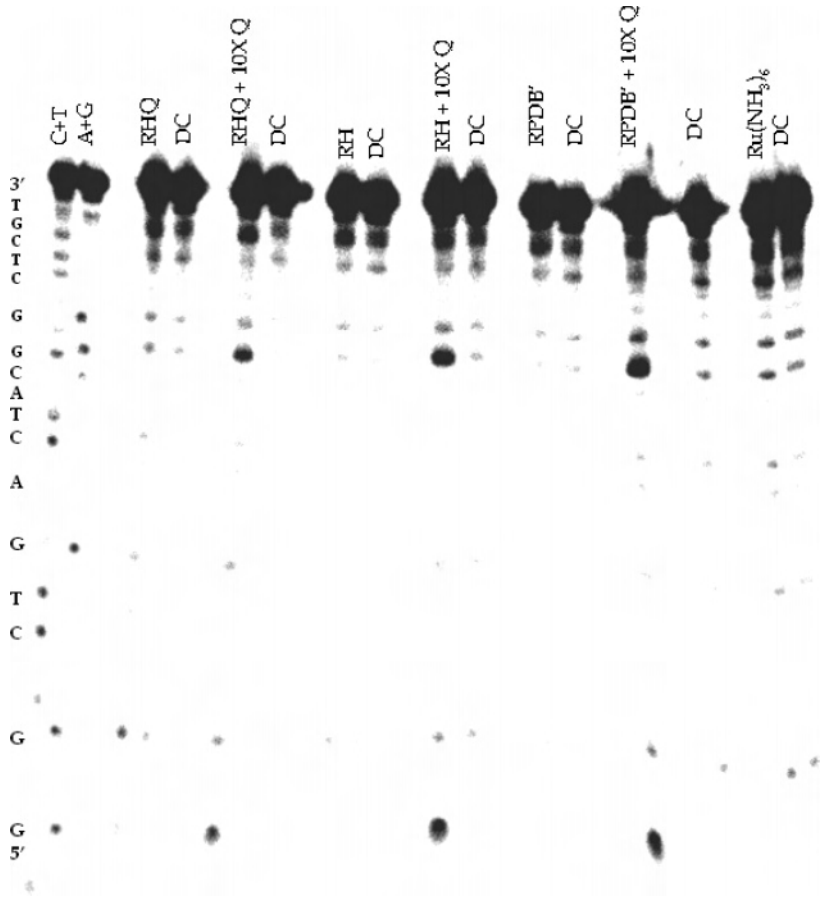

Figure 5. Phosphorimagry following gel electrophoretic analysis of the sequence 3′-TGCTCGGCATCAGTCGGCATA-5′ after irradiation and piperidine treatment in the presence of the ruthenium complexes $[Ru(phen)(dppz)(bpy')]^{2+}$ (RPDB′), $[Ru(phen)(dppz)(bpy'\text{-his})]^{2+}$ (RH), and $[\{Ru(phen)(dppz)(bpy'\text{-his})\}\{Ru(NH_3)_5\}]^{5+}$ (RHQ). Also shown are the same complexes with added $[Ru(NH_3)_6]^{3+}$ quencher (Q). Dark control (DC) samples containing DNA and metal were not irradiated. All other samples were irradiated for 30 min using an excitation wavelength of 442 nm. Samples contained 4 μM duplex DNA, 4 μM ruthenium complex, and 40 μM $[Ru(NH_3)_6]^{3+}$ if added.

Recently our laboratory has observed oxidative ring-opening of a cyclopropylcytosine trap in DNA, consistent with transient hole occupation on pyrimidines.[22] Reductive ring opening was also observed using this system with a platinum complex.[49] As can be seen in Figure 6, neither $[\{Ru(phen)(dppz)(bpy'\text{-his})\}\{Ru(NH_3)_5\}]^{5+}$ nor $[Ru(phen)(dppz)(bpy'\text{-his})]^{2+}$ and $[Ru(phen)(dppz)(bpy')]^{2+}$ are capable of opening the ^{CP}C ring by oxidation or reduction, as we would expect based on their electrochemical potentials versus those of ^{CP}C (Table 3).

EPR Spectroscopy. We have established that $[\{Ru(phen)(dppz)(bpy'\text{-his})\}\{Ru(NH_3)_5\}]^{5+}$ can facilitate CPG ring opening when noncovalently bound to duplex DNA. To probe this reaction further, we used EPR to detect the guanine radical spectroscopically.[50] As shown in Figure 7, $[\{Ru(phen)(dppz)(bpy'\text{-his})\}\{Ru(NH_3)_5\}]^{5+}$ in the presence of poly-d(GC) shows a small signal with $g = 2.004$, comparable to that of the guanine radical.[51] This signal is not evident for $[\{Ru(phen)(dppz)(bpy'\text{-his})\}\{Ru(NH_3)_5\}]^{5+}$ in the presence of poly-d(AT), further consistent with the assignment of the signal to a guanine radical rather than a histidine radical.[52] It should also be noted that this result is also consistent with previous findings that flash-quench methodologies using $[Ru(phen)_2(dppz)]^{3+}$ do not generate adenine radical cations.[50]

Nanosecond Transient Absorption Spectroscopy. In addition to EPR spectroscopy, transient absorption spectroscopy can be used to detect guanine radical formation using the flash-quench technique. We examined the spectroscopic characteristics of $[\{Ru(phen)(dppz)(bpy'\text{-his})\}\{Ru(NH_3)_5\}]^{5+}$ and $[Ru(phen)(dppz)(bpy'\text{-his})]^{2+}$ in the presence and absence of DNA (Figure 8). Inspection of the data in Figure 8A, which compares the behavior of the two complexes in poly-d(AT), shows an initial bleach at 440 nm corresponding to the Ru(II) excited state. For $[Ru(phen)(dppz)(bpy'\text{-his})]^{2+}$, in the absence of $[Ru(NH_3)_6]^{3+}$ quencher, this bleach decays back to baseline within the excited state lifetime. In the presence of quencher, a longer-lived negative absorbance following the initial bleach is observed and is consistent with formation of Ru(III), which like Ru(II)*, absorbs less at 440 nm than does ground state Ru(II). In contrast, [{Ru(phen)-

(49) Lu, W.; Vicic, D. A.; Barton, J. K. *Inorg. Chem.* **2005**, *22*, 7970−7980.
(50) Schiemann, O.; Turro, N. J.; Barton, J. K. *J. Phys. Chem. B* **2000**, *104*, 7124−7220.
(51) Yavin, E.; Boal, A. K.; Stemp, E. D. A.; Boon, E. M.; Livingston, A. L.; O'Shea, V. L.; David, S. S.; Barton, J. K. *Proc. Natl. Acad. Sci. U.S.A.* **2005**, *102*, 3546−3551.
(52) Berthomieu, C.; Boussac, A. *Biochemistry* **1995**, *34*, 1541.
(53) Cullis, P. M.; Malone, M. E.; Merson-Davies, L. A. *J. Am. Chem. Soc.* **1996**, *118*, 2775−2781.

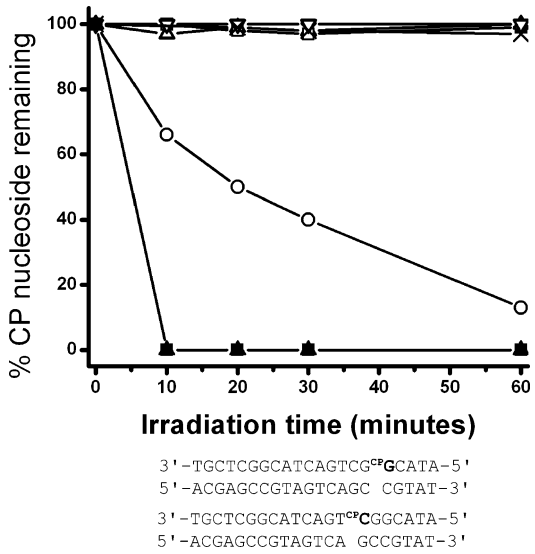

Figure 6. Decomposition of ^{CP}G in the G-2 duplex (upper sequence) as a function of irradiation time in the presence of [{Ru(phen)(dppz)(bpy′-his)}{Ru(NH$_3$)$_5$}]$^{5+}$ (○), [Ru(phen)(dppz)(bpy′)]$^{2+}$ (△), [Ru(phen)(dppz)(bpy′-his)]$^{2+}$ (□), [Ru(phen)(dppz)(bpy′)]$^{2+}$ + [Ru(NH$_3$)$_6$]$^{3+}$ (▲), [Ru(phen)(dppz)(bpy′-his)]$^{2+}$ + [Ru(NH$_3$)$_6$]$^{3+}$ (■), and [Ru(phen)(dppz)(bpy′-his)]$^{2+}$ at pH 5 (▽). Also shown in the effect of irradiation on ^{CP}C in the C-1 duplex (lower sequence) in the presence of [{Ru(phen)(dppz)(bpy′-his)}{Ru(NH$_3$)$_5$}]$^{5+}$ (X). All experiments were done under anaerobic conditions using an excitation wavelength of 442 nm. Experiments were done in 10 mM sodium phosphate, 50 mM NaCl, pH 7 in the presence of 5 μM duplex, 5 μM ruthenium complex and 100 μM [Ru(NH$_3$)$_6$]$^{3+}$. The experiment at low pH was done in 10 mM NaOAc, 50 mM NaCl, pH 5. See Experimental Section.

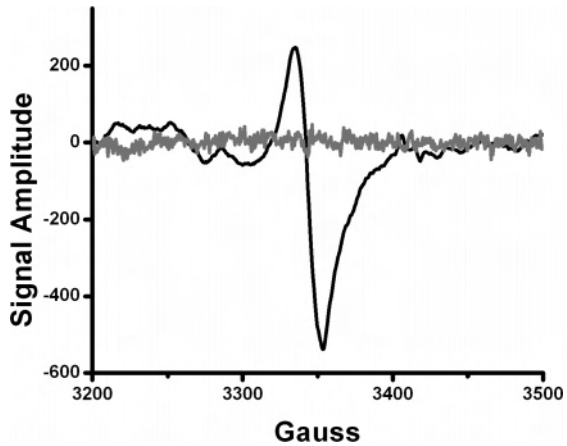

Figure 7. Guanine radical formation by [{Ru(phen)(dppz)(bpy′-his)}{Ru(NH$_3$)$_5$}]$^{5+}$. EPR spectra measured at 20 K of 0.1 mM [{Ru(phen)(dppz)(bpy′-his)}{Ru(NH$_3$)$_5$}]$^{5+}$ in 1.5 mM poly d(AT) (light gray trace) or poly d(GC) (black trace). Buffer was composed of 10 mM sodium phosphate, 50 mM NaCl, pH 7. See Experimental Section.

(dppz)(bpy′-his)}{Ru(NH$_3$)$_5$}]$^{5+}$, in the absence of quencher, yields a long-lived positive signal following the excited state bleach at 440 nm. The signal forms faster than the detection limit of the instrument (formation rate with a lower limit of $\sim 10^8$ s^{-1}). As can be seen in Figure 8B, the magnitude of this signal is larger in poly-d(AT) than in poly-d(GC), and this positive signal is not evident in acetonitrile in the absence of DNA. As with [Ru(phen)(dppz)(bpy′-his)]$^{2+}$, when quencher is added to Ru(phen)(dppz)(bpy′-his)}{Ru(NH$_3$)$_5$}]$^{5+}$, a long-lived negative absorbance follows the initial excited state bleach, indicative of Ru(III) formation (Figure 8B).

Figure 9A shows a difference spectrum obtained for [{Ru(phen)(dppz)(bpy′-his)}{Ru(NH$_3$)$_5$}]$^{5+}$ with both DNA polymers. This spectrum markedly contrasts with the difference spectrum obtained for [Ru(phen)(dppz)(bpy′-his)]$^{2+}$ in poly-d(AT) in the presence and absence of quencher (Figure 9A inset). The long-lived transient formed in [{Ru(phen)(dppz)(bpy′-his)}{Ru(NH$_3$)$_5$}]$^{5+}$ in both poly-d(AT) and poly-d(GC) contains two positive extrema, centered at 410 and 560 nm. The magnitude of the transient is larger in poly-d(AT) than that in poly-d(GC), as would be expected on the basis of the single-wavelength transients at 440 nm. In contrast, the difference spectra for the Ru(II)*/Ru(II) and Ru(III)/Ru(II) transitions generated from excitation of [Ru(phen)(dppz)(bpy′-his)]$^{2+}$ in poly-d(AT) in the presence and absence of quencher are notably negative at 440 nm in the MLCT region. Figure 9B shows a difference spectrum of excited [Ru(phen)(dppz)(bpy′-his)]$^{2+}$ in the presence of the reductive quencher, ascorbate. This Ru(II)*/Ru(I) transition thus generates a transient with positive extrema at 400 and 410 nm. In a manner similar to that of the [{Ru(phen)(dppz)(bpy′-his)}{Ru(NH$_3$)$_5$}]$^{5+}$ spectrum, there is a negative region between 350 and 360 nm.

Charge Effect on the Transient Absorption Profile of [Ru(phen)(dppz)(bpy′-his)]$^{2+}$ in DNA. To further probe the long-lived transient species formed upon excitation of [{Ru(phen)(dppz)(bpy′-his)}{Ru(NH$_3$)$_5$}]$^{5+}$ in the presence of both DNA polymers, we investigated the effect of a positive charge on the imidazole ring of [Ru(phen)(dppz)(bpy′-his)]$^{2+}$. We examined the transient absorption profiles of [Ru(phen)(dppz)(bpy′-his)]$^{2+}$ in the presence of positively charged coordinating species such as Zn^{2+} and [Ru(NH$_3$)$_5$(H$_2$O)]$^{2+}$, as well as at a pH lower than the pK_a of histidine to determine if we could mimic the environment of the charged imidazole in [{Ru(phen)(dppz)(bpy′-his)}{Ru(NH$_3$)$_5$}]$^{5+}$. At pH 5, the transient absorption of [Ru(phen)(dppz)(bpy′-his)]$^{2+}$ in the presence of poly-d(AT) shows a strong positive signal at 440 nm, while in poly-d(GC), the signal is above baseline (Figure 8C). Note that at pH 7, this positive signal is not apparent. The emission of [Ru(phen)(dppz)(bpy′-his)]$^{2+}$ as monitored at 620 nm is not quenched in intensity or lifetime as a result of lowered pH (data not shown). In contrast, when measurements were taken in the presence of 2.5 mM Zn^{2+} or 0.3 mM [Ru(NH$_3$)$_5$(H$_2$O)]$^{2+}$, no change in the [Ru(phen)(dppz)(bpy′-his)]$^{2+}$ transient absorption spectrum is observed (Figure 8D). Interestingly, [Ru(NH$_3$)$_5$(H$_2$O)]$^{2+}$ has a small quenching effect on the excited-state lifetime of [Ru(phen)(dppz)(bpy′-his)]$^{2+}$ in 1 mM poly-d(AT). This effect is not seen in the presence of Zn^{2+}(data not shown). Perhaps neither coordinate significantly with the complex already bound to DNA.

As can be seen in Figure 6, ^{CP}G ring opening is not observed when [Ru(phen)(dppz)(bpy′-his)]$^{2+}$ at pH 5 is used as the photooxidant suggesting that the transient formed spectroscopically is not responsible for the oxidation process. This is consistent with the time-resolved and steady-state emission data at pH 5, which show no increase in quenching at lower pHs.

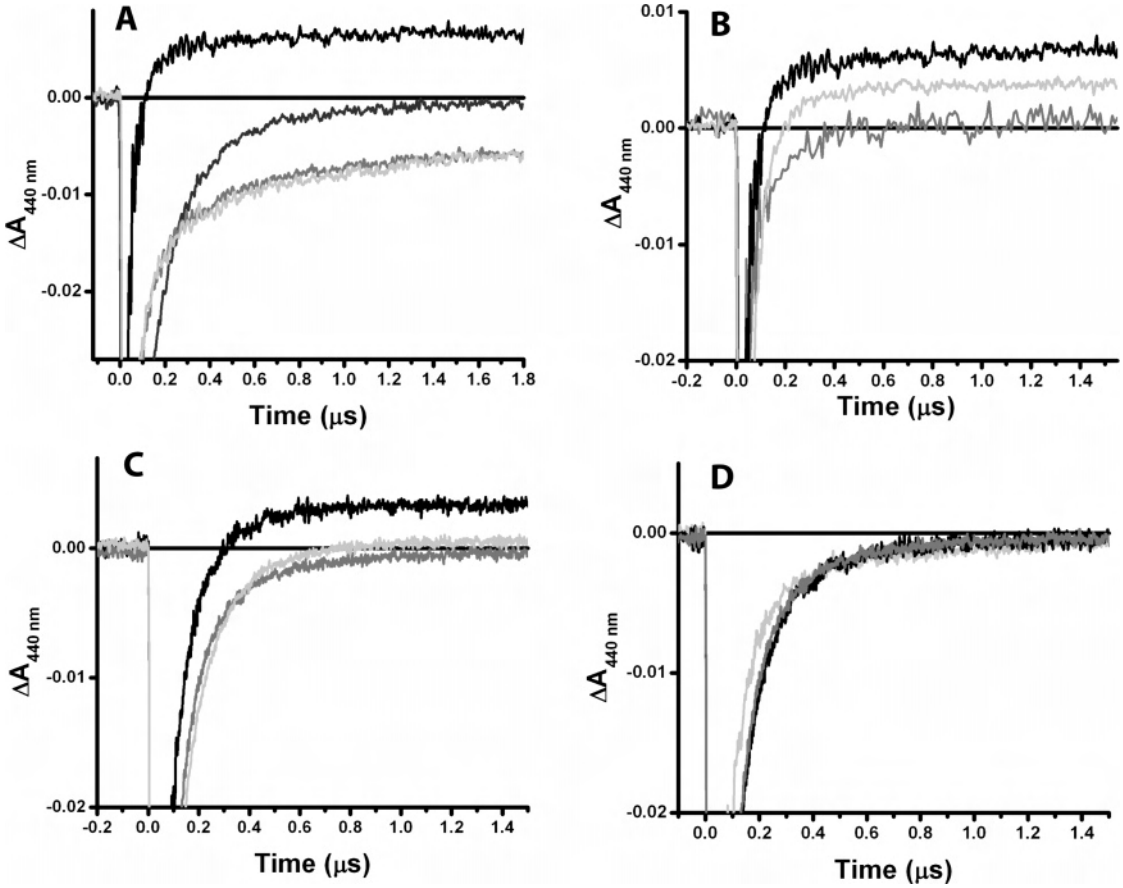

Figure 8. Transient absorption at 440 nm of the ruthenium complexes. A shows $[\{Ru(phen)(dppz)(bpy'\text{-}his)\}\{Ru(NH_3)_5\}]^{5+}$ and $[Ru(phen)(dppz)(bpy'\text{-}his)]^{2+}$ in the presence (gray and light gray traces, respectively) and absence (black and dark gray traces, respectively) of $[Ru(NH_3)_6]^{3+}$ measured in 1 mM poly-d(AT) in 10 mM sodium phosphate, 50 mM NaCl, pH 7.0. A comparison of the $[\{Ru(phen)(dppz)(bpy'\text{-}his)\}\{Ru(NH_3)_5\}]^{5+}$ signal in 1 mM poly d(AT) (black trace) or poly-d(GC) (light gray trace) and acetonitrile (gray trace) is shown in B. The effect of lowered pH on the $[Ru(phen)(dppz)(bpy'\text{-}his)]^{2+}$ 440 nm signal is examined in C. The black and light gray traces correspond to $[Ru(phen)(dppz)(bpy'\text{-}his)]^{2+}$ in the presence of 1 mM poly-d(AT) and poly-d(GC), respectively, in 10 mM NaOAc, 50 mM NaCl, pH 5. The gray trace corresponds to $Ru(phen)(dppz)(bpy'\text{-}his)]^{2+}$ in 1 mM poly-d(AT) in 10 mM sodium phosphate, 50 mM NaCl, pH 7. D shows the effect of adding 2.5 mM Zn^{2+} (black trace) and 0.3 mM $[Ru(NH_3)_5(H_2O)]^{2+}$ (light gray trace) to $[Ru(phen)(dppz)(bpy'\text{-}his)]^{2+}$ in the presence of 1 mM poly-d(AT) in 10 mM sodium phosphate, 50 mM NaCl, pH 7. The gray trace of $[Ru(phen)(dppz)\text{-}(bpy'\text{-}his)]^{2+}$ in 1 mM poly-d(AT) in 10 mM sodium phosphate, 50 mM NaCl, pH 7 is shown for comparison. Experiments were done using 30 μM ruthenium complex and 300 μM $[Ru(NH_3)_6]^{3+}$ as the quencher. See Experimental Section.

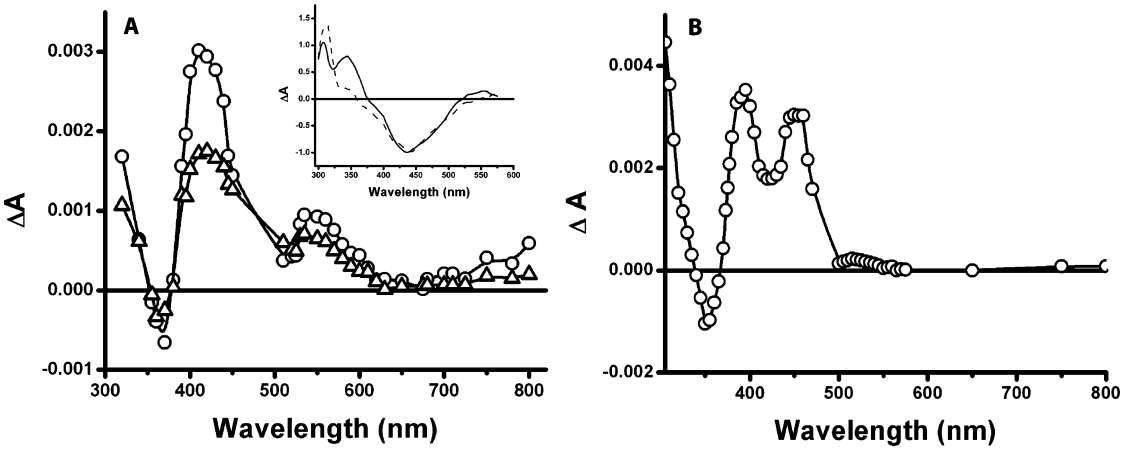

Figure 9. (A) Transient absorption difference spectrum for 30 μM $[\{Ru(phen)(dppz)(bpy'\text{-}his)\}\{Ru(NH_3)_5\}]^{5+}$ in 1 mM poly-d(GC) (△) and poly-d(AT) (○). The inset shows difference spectra for 30 μM $[Ru(phen)(dppz)(bpy'\text{-}his)]^{2+}$ in poly-d(AT) with (- -) and without (—) 300 μM $[Ru(NH_3)_6]^{3+}$. Samples were measured in 10 mM sodium phosphate, 50 mM NaCl, pH 7. **(B)** Transient absorption difference spectrum for 30 μM $[Ru(phen)(dppz)(bpy'\text{-}his)]^{2+}$ in the presence of 25 mM ascorbate measured in acetonitrile.

Emission Characteristics of $[\{Ru(phen)(dppz)(bpy'\text{-}his)\}\{Ru(NH_3)_5\}]^{5+}$, $[Ru(phen)(dppz)(bpy'\text{-}his)]^{2+}$ and $[Ru(phen)(dppz)(bpy')]^{2+}$. $[\{Ru(phen)(dppz)(bpy'\text{-}his)\}\text{-}\{Ru(NH_3)_5\}]^{5+}$, a ruthenium complex with a tethered quencher, is capable of oxidizing guanine bases in DNA without an added quencher. On the basis of steady-state and time-resolved emission spectroscopy, $[\{Ru(phen)(dppz)(bpy'\text{-}his)\}\{Ru(NH_3)_5\}]^{5+}$ is significantly quenched relative to

$[Ru(phen)(dppz)(bpy'\text{-}his)]^{2+}$ and $[Ru(phen)(dppz)(bpy')]^{2+}$ in DNA and organic solvents, as would be expected if an external quencher, such as $[Ru(NH_3)_6]^{3+}$, is present.

Transient absorption and time-resolved emission measurements indicate that, although the excited-state lifetime of the $[\{Ru(phen)(dppz)(bpy'\text{-}his)\}\{Ru(NH_3)_5\}]^{5+}$ complex is drastically reduced relative to the parent complexes, formation of Ru(III) is not observable on the time scale of our measurement, suggesting that back electron transfer with the reduced quencher is a dominant pathway for this complex. Charge recombination is not surprising in this system, given that the quencher is in close proximity to the ruthenium center. Indeed, an initial benefit of the original flash-quench technique was spatial separation of charge between the quencher and ruthenium complex, thus reducing the probability of back electron transfer. Because there is covalent coupling between the two metal centers in the $[\{Ru(phen)(dppz)(bpy'\text{-}his)\}\{Ru(NH_3)_5\}]^{5+}$ complex, the rate of back electron transfer is enhanced.

Guanine Radical Formation with $[\{Ru(phen)(dppz)(bpy'\text{-}his)\}\{Ru(NH_3)_5\}]^{5+}$. A long-lived charge-separated state is requisite for the formation of permanently damaged DNA oxidation products, because the oxidized ruthenium must persist long enough for charge injection to occur within the duplex. These long-lived charge separated states are most often attained by ensuring that the driving force for charge recombination lies in the Marcus inverted region[54] or by spatially separating the donor and acceptor. We have demonstrated that we cannot measure guanine damage by gel electrophoresis using the $[\{Ru(phen)(dppz)(bpy'\text{-}his)\}\{Ru(NH_3)_5\}]^{5+}$ complex because the millisecond trapping rate of guanine radical is much slower than the rate of back electron transfer from the reduced quencher. Contributions from back electron transfer to guanine oxidation can be eliminated, however, by using a kinetically fast hole trap, which opens irreversibly upon oxidation on a time scale of 10^{-11} s. By using such a system, we can probe charge-transfer events between $[\{Ru(phen)(dppz)(bpy'\text{-}his)\}\{Ru(NH_3)_5\}]^{5+}$ and DNA, which are not apparent on the slow time scale of guanine radical trapping. Indeed, when $[\{Ru(phen)(dppz)(bpy'\text{-}his)\}\{Ru(NH_3)_5\}]^{5+}$ is irradiated in the presence of duplex DNA containing a ^{CP}G hole trap, ring opening is observed, consistent with charge injection by the complex into the DNA.

Interestingly, the efficiency of ^{CP}G ring opening is less for $[\{Ru(phen)(dppz)(bpy'\text{-}his)\}\{Ru(NH_3)_5\}]^{5+}$ than for a complex with added quencher, suggesting that back electron transfer is still competitive with charge injection or that there are other competitive pathways. Traditional flash-quench methodologies use a diffusible quencher, which despite limiting the rate of quenching, can freely diffuse on the time scale of Ru(II) excited state decay, creating a spatial separation of charge and a decreased rate of back electron transfer. In contrast, in the case of $[\{Ru(phen)(dppz)(bpy'\text{-}his)\}\{Ru(NH_3)_5\}]^{5+}$, the reduced quencher moiety cannot freely diffuse, so back electron transfer remains a competing pathway.

We can spectroscopically detect guanine radical formation generated by excitation of $[\{Ru(phen)(dppz)(bpy'\text{-}his)\}\{Ru(NH_3)_5\}]^{5+}$ using EPR. Consistent with guanine oxidation by ^{CP}G ring opening, we find that when a sample containing $[\{Ru(phen)(dppz)(bpy'\text{-}his)\}\{Ru(NH_3)_5\}]^{5+}$ in poly-d(GC) is irradiated while simultaneously freezing in liquid nitrogen, an organic radical is detectable by EPR. At lower temperatures, the rate of back electron transfer is slower and therefore not competitive with guanine radical formation. This radical resembles that of the neutral guanine radical seen in previous experiments.[51,53] This radical does not form in sequences lacking guanines or when $[Ru(phen)(dppz)(bpy'\text{-}his)]^{2+}$ is irradiated in the absence of quencher in guanine-containing duplexes, consistent with intramolecular flash-quench generated oxidation by $[\{Ru(phen)(dppz)(bpy'\text{-}his)\}\{Ru(NH_3)_5\}]^{5+}$ to first form the dppz complex of Ru(III) that can then oxidize guanine.

Transient Species Formed in the Presence of DNA. Although $[\{Ru(phen)(dppz)(bpy'\text{-}his)\}\{Ru(NH_3)_5\}]^{5+}$ is capable of oxidizing guanine in DNA, it is apparent that competing processes exist that contribute to diminished ^{CP}G decomposition efficiency and the lack of a prominent guanine radical as detected by transient absorption spectroscopy. As can be seen in Figure 9A, a new species is formed when $[\{Ru(phen)(dppz)(bpy'\text{-}his)\}\{Ru(NH_3)_5\}]^{5+}$ is irradiated in the presence of both DNA polymers and its signal is strong enough to obscure the detection of any guanine radicals formed in the experiment. This long-lived species persists on the millisecond time scale and requires DNA; the species is not detected in acetonitrile. Although this transient is formed immediately following the initial excited-state bleach at 440 nm, it is not necessary for the oxidation of DNA. Indeed, $[Ru(phen)(dppz)(bpy'\text{-}his)]^{2+}$ without the coordinated $[Ru(NH_3)_5]^{3+}$, at pH values lower than the pK_a of histidine, yields an analogous transient, albeit on a slower time scale, but it does not oxidize guanine as measured by ^{CP}G ring opening. Moreover, the excited-state lifetime of $[Ru(phen)(dppz)(bpy'\text{-}his)]^{2+}$ is unaltered by this pH change, and the steady-state emission shows no quenching. Thus, an extremely short-lived Ru(III) species coordinated to dppz must exist in $[\{Ru(phen)(dppz)(bpy'\text{-}his)\}\{Ru(NH_3)_5\}]^{5+}$, which is not detectable on the time scale of the measurement and is not required for the formation of the positive transient.

A positive charge on the histidine imidazole is required for formation of the long-lived transient formed in $[\{Ru(phen)(dppz)(bpy'\text{-}his)\}\{Ru(NH_3)_5\}]^{5+}$ and $[Ru(phen)(dppz)(bpy'\text{-}his)]^{2+}$ at low pH. The transient is not formed with $[Ru(phen)(dppz)(bpy')]^{2+}$ at low pH because this complex does not contain a histidine moiety. Given that a protonated histidine on $[Ru(phen)(dppz)(bpy'\text{-}his)]^{2+}$ will lead to the formation of the long-lived transient, we wondered if a positively charged coordinating metal would exhibit similar behavior. However, neither Zn^{2+} nor $[Ru(NH_3)_5(H_2O)]^{2+}$

(54) (a) Gould, I. R.; Moser, J. E.; Armitage, B.; Farid, S. *J. Am. Chem. Soc.* **1989**, *111*, 1917−1919. (b) Marcus, R. A. *J. Phys. Chem.* **1956**, *24*, 966−978.

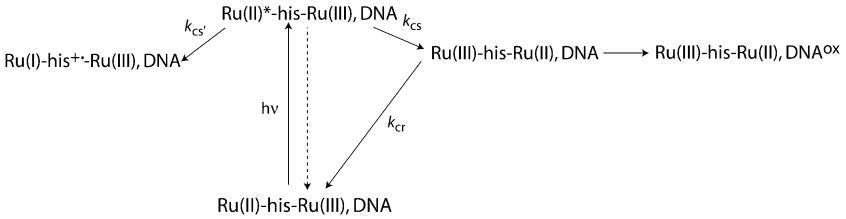

Figure 10. Scheme illustrating the various photophysical pathways for $[\{Ru(phen)(dppz)(bpy'\text{-}his)\}\{Ru(NH_3)_5\}]^{5+}$ in the presence of DNA. Excitation into its MLCT results in the excited-state ruthenium(II) species, which can either undergo the standard flash-quench pathway resulting in the ground state oxidant Ru(III) or it can accept an electron from the nearby histidine resulting in a reduced ruthenium center and an oxidized histidine stabilized by the positive ruthenium pentammine quencher.

facilitates formation of the long-lived transient. Possibly, in the presence of DNA, neither specifically coordinates to the histidine.

Competing Photophysical Pathways of $[\{Ru(phen)(dppz)(bpy'\text{-}his)\}\{Ru(NH_3)_5\}]^{5+}$ in a DNA Environment. The long-lived transient species detected when $[\{Ru(phen)(dppz)(bpy'\text{-}his)\}\{Ru(NH_3)_5\}]^{5+}$ is irradiated in the presence of DNA bears striking resemblance to that of a reduced ruthenium species.[55] To compare the chemical formation of Ru(I) with the transient observed in our system, we examined the spectrum of $[Ru(phen)(dppz)(bpy'\text{-}his)]^{2+}$ in the presence of the reductive quencher, ascorbate. When ruthenium(II) polypyridyl complexes are irradiated in its presence, a long-lived transiently generated Ru(I) species is obtained (Figure 9B). Interestingly, Ru(I), as monitored by transient absorption, shows similar features to the transient generated by irradiation of $[\{Ru(phen)(dppz)(bpy'\text{-}his)\}\{Ru(NH_3)_5\}]^{5+}$ or $[Ru(phen)(dppz)(bpy'\text{-}his)]^{2+}$ at pH 5 in the presence of DNA. A small negative region spans the area between ~330 and 365 nm, and maxima exist around 410−440, 530, and <320 nm. The Ru(I) formed by reductive quenching with ascorbate yields a spectrum with a small dip in between the maxima at 410 and 440 nm, which is likely the result of a small amount of Ru(III) present in the sample (Figure 9A). In contrast, the spectra generated by reductive quenching of $[\{Ru(phen)(dppz)(bpy'\text{-}his)\}\{Ru(NH_3)_5\}]^{5+}$ and $[Ru(phen)(dppz)(bpy'\text{-}his)]^{2+}$ do not appear to have Ru(III) interference.

This transient spectrum we see for $[\{Ru(phen)(dppz)(bpy'\text{-}his)\}\{Ru(NH_3)_5\}]^{5+}$ in DNA resembles very closely that of a reduced $[Ru(bpy)_2(bpz)]^{2+}$ complex (bpz = 2,2′-bipyrazine) generated by pulse radiolysis.[55] It should be noted, however, that the spectrum of the reduced complex generated electrochemically bears no resemblance to that generated using transient absorption.[56,57] However, electrochemically reducing the complex results in subsequent reductions of each ligand, leaving the metal center unaffected.

Mechanistic Considerations. As shown in Figure 10, we propose a model in which, upon excitation into its MLCT band in the presence of DNA, $[\{Ru(phen)(dppz)(bpy'\text{-}his)\}\{Ru(NH_3)_5\}]^{5+}$ can undergo two different reaction pathways. The first pathway is the standard flash-quench route, in which the excited-state is quenched by neighboring $[Ru(NH_3)_5\text{-}(His)]^{3+}$ to generate the powerful ground state oxidant, Ru(III). With a potential of 1.5 V, Ru(III) can oxidize guanine. Because the reduced quencher is not spatially separated from the newly generated Ru(III) oxidant, back electron transfer is a dominant pathway through which Ru(III) is able to return to the ground state.

The second pathway occurs when the $[\{Ru(phen)(dppz)(bpy'\text{-}his)\}\{Ru(NH_3)_5\}]^{5+}$ excited state accepts an electron from the nearby histidine thus resulting in a polarized complex, forming a ligand radical coordinated to the Ru(I) center. Although $RuL^{\bullet+}$ species are effective reducing agents, they are not capable of reducing the bases of DNA.[55] It is interesting to note that this phenomenon occurs only when the complex is intercalated into the DNA polyanion; this species does not form in acetonitrile. The DNA is thus able to orient the complex in a stable polarized form, such that the ruthenium center is reduced, while the histidine moiety is oxidized. The negatively charged DNA is essential to this chemistry. Although it may theoretically be possible for the histidine cation radical, with a potential of ~1.3 V[59] to abstract an electron from guanine (1.3 V), it is highly unlikely because of the less-favorable driving force compared with oxidation by Ru(III) (1.5 V). In addition, the reaction would be sterically hindered because the histidine is kept a significant distance from the DNA by the bpy′ ligand when the dppz ligand is intercalated.

The characterization of $[\{Ru(phen)(dppz)(bpy'\text{-}his)\}\{Ru(NH_3)_5\}]^{5+}$ allows us to observe a variety of electron transfer pathways that can occur only in the presence of DNA. Not only can this complex undergo intramolecular charge transfer between the quencher and the ruthenium(II) excited state on picosecond time scales, but a competing charge transfer event can occur between the ruthenium(II) excited state and the histidine bridge, which persists on a millisecond time scale. It should be noted that it is the presence of a positive charge on, rather than the redox state of the quencher, that allows these additional pathways to occur. Moreover, this unique behavior is only possible when the complex is properly oriented in a sea of polyanionic DNA which can stabilize the positive charge localized on the histidine. This system underscores the rich electron-transfer chemistry of ruthenium

(55) D'angelantonio, M.; Mulazzani, Q. G.; Venturi, M.; Ciano, M.; Hoffman, M. Z. *J. Phys. Chem.* **1991**, *95*, 5121−5129.
(56) Fees, J.; Ketterle, M.; Klein, A.; Fiedler, J.; Kaim, W. *J. Chem. Soc., Dalton Trans.* **1999**, 2595−2599.
(57) Fees, J.; Kaim, W.; Moscherosch, M.; Matheis, W.; Klima, J.; Krejcik, M.; Zalis, S. *Inorg. Chem.* **1993**, *32*, 166−174.
(58) Arkin, M. R.; Stemp, E. D. A.; Turro, C.; Turro, N. J.; Barton, J. K. *J. Am. Chem. Soc.* **1996**, *118*, 2267−2274.
(59) Iwunze, M. O. *Bull. Electrochem.* **2005**, *21*, 555−560.

and allows us to observe novel pathways in which electrons and holes can migrate between two metal centers bound to DNA.

Acknowledgment. We are grateful to the NIH for their financial support. We also thank M.C. DeRosa and E. Yavin for technical assistance.

Supporting Information Available: Extinction coefficients for DNA sequences, electrospray ionization mass spectrum of {Ru(phen)(dppz)(bpy′-his)}{$Ru(NH_3)_5$}$]^{5+}$, HPLC traces and absorbance profiles for the three complexes [Ru(phen)(dppz)(bpy′)]$^{2+}$, [Ru(phen)(dppz)(bpy′-his)]$^{2+}$, and [{Ru(phen)(dppz)(bpy′-his)}{$Ru(NH_3)_5$}$]^{5+}$, HPLC traces following irradiation of [{Ru(phen)(dppz)(bpy′-his)}{$Ru(NH_3)_5$}$]^{5+}$ in acetonitrile, and electrochemical oxidation profiles for [Ru(phen)(dppz)(bpy)]$^{2+}$ and [Ru(phen)(dppz)(bpy′-his)]$^{2+}$. This material is available free of charge via the Internet at http://pubs.acs.org.

IC701276T